

Original article

Influence of the aperture area on the performance of a solar funnel cooker operating at high sun elevations using glycerine as load

Celestino Rodrigues Ruivo^{a,b,*}, Xabier Apaolaza-Pagoaga^c, Antonio Carrillo-Andrés^c, Gianluca Coccia^d^a Department of Mechanical Engineering, Institute of Engineering, University of Algarve, Portugal^b ADAI – LAETA, Rua Pedro Hispano n° 12, 3030-289 Coimbra, Portugal^c Energy Research Group, Department of Mechanical, Thermal and Fluids Engineering, University of Malaga, Calle Arquitecto Francisco Peñalosa, 6, 29071 Malaga, Spain^d Marche Polytechnic University, Department of Industrial Engineering and Mathematical Sciences, Via Breccia Bianche 12, 60131 Ancona, Italy

ARTICLE INFO

Keywords:

Solar cooking
Funnel cooker
Experimental test
Side-by-side
Reflective surface area

ABSTRACT

Five funnel solar cookers have been tested to investigate the influence of the aperture area on their performance. The largest cooker had an aperture area of 0.5 m² and it was tested side by side with two other two smaller cookers. Each cooker was tested with the same amount of glycerine.

The linear performance curves relating the efficiency with the specific temperature difference was determined. Then, the determined regressions of the cooker opto-thermal ratio and the reference time on the aperture area were used to predict: i) the influence of the solar irradiance and the aperture area on the maximum temperature achieved by the load, ii) the time duration required for achieving load temperature from 65 to 140 °C, and iii) the power of the cooker. It was found that for a solar irradiance range of 600–1100 W m⁻², the pasteurization temperature can be achieved even by the smallest cooker, and the efficiency of the largest cooker is close to the efficiency of a cooker with optimum aperture area. Moreover, when using the largest cooker, under an irradiance of 1100 W m⁻² and ambient temperature 20 °C, the load can achieve 180 °C, implying that frying is possible.

Introduction

Solar cookers are usually used for cooking food and making hot beverages, but they can also be used for water pasteurization and other important tasks when operated during periods of the day with good incoming solar radiation. Many solar cooker designs have been developed in the last few decades, making it difficult to classify all of them in groups. However, they are usually classified into four main groups: panel cookers, box cookers, tube cookers and parabolic cookers.

Most common parabolic dish solar cookers are able to cook food as readily as a gas burner. From tests conducted at intermediate temperature, when using cookers with medium aperture area under good solar radiation conditions, the maximum achievable load temperature is estimated to be in the range of 170 °C to 250 °C, depending on the cooker, pot and load used [1,2]. When solar radiation is weak, cooking using cookers with average aperture area may be possible if a transparent heat trap around the pot is used. In case of parabolic dish cookers with small aperture area, such transparent heat trap around the pot is

required to speed up the cooking process. According to recent conducted tests, the maximum achievable load temperature, when using a small deep parabolic solar cooker without heat trap, was estimated to be in around 115 °C [2], which is similar to the value obtained experimentally when testing a new solar cooker named as “Quonset solar cooker” [3]. Besides this, another new design of solar cooker having the cooking chamber equipped with internal reflectors and a bottom cylindrical parabolic reflector was tested. It resulted in the maximum values of achievable load temperature 124 °C and 144 °C, respectively, when not using and using the bottom parabolic reflector [4].

Some funnel solar cooker designs have been developed and used in the last decades for direct solar cooking [5]. The aperture area to collect solar radiation of most of the designs of funnel solar cookers is relatively low. Thus, a transparent glass enclosure acting as a heat trap, i.e., making a greenhouse effect around the cooking vessel, is commonly adopted to ensure the success of cooking food items, in sunny days, at slow or medium cooking speed, depending on the mass of the food to be cooked. Some of the developed designs have a set of multiple reflecting elements with a shape equivalent to a funnel.

* Corresponding author.

E-mail address: cruivo@ualg.pt (C.R. Ruivo).<https://doi.org/10.1016/j.seta.2022.102600>

Received 9 May 2022; Received in revised form 16 July 2022; Accepted 31 July 2022

Available online 8 August 2022

2213-1388/© 2022 The Authors. Published by Elsevier Ltd. This is an open access article under the CC BY license (<http://creativecommons.org/licenses/by/4.0/>).

Nomenclature			
$A_{n,max}$	Maximum normal area to the sun rays being collected by the solar cooker (m^2)	$t_{i,f}$	Time required to change load temperature from $T_{f,i}$ to $T_{f,f}$ (s)
A_{ref}	Effective reflector area (m^2)	t_{ref}	Reference time (s)
c_f	Specific heat of load ($J\ ^\circ C^{-1}\ kg^{-1}$)	w_c	Width of the strip (m)
COR	Cooker opto-thermal ratio ($^\circ C\ m^2\ W^{-1}$)	w_p	Width of rectangular part of the reflector plate (m)
I_n	Global normal solar irradiance, i.e., global solar irradiance on the plane normal to beam radiation ($W\ m^{-2}$)	Greek symbols	
$I_{n,exp,i}$	Average global normal solar irradiance at time interval i ($W\ m^{-2}$)	χ	Specific temperature difference ($^\circ C\ m^2\ W^{-1}$)
\bar{I}_n	Average global normal solar irradiance during a test ($W\ m^{-2}$)	$\chi_{exp,i}$	Specific temperature difference at time interval i ($^\circ C\ m^2\ W^{-1}$)
l_p	Effective side length of the square part or effective length of rectangular part of the reflector plate (m)	χ_{max}	Maximum value of the specific temperature difference ($^\circ C\ m^2\ W^{-1}$)
m_f	Mass of load (kg)	Δt_i	Duration of time interval i (s)
n_p	Number of observation points	$\Delta T_{f,exp,i}$	Variation of load temperature at time interval i ($^\circ C$)
\dot{Q}	Cooker power (W)	$\Delta T_{f,a}$	Difference between load temperature and ambient temperature ($^\circ C$)
\dot{Q}_0	Cooker power for $\Delta T_{f,a} = 0\ ^\circ C$ (W)	$\Delta T_{f,a,max}$	Maximum value of the difference between load temperature and ambient temperature ($^\circ C$)
\dot{Q}_{Tf}	Power of cooker when load temperature is T_f (W)	$\Delta T_{f,a,exp,i}$	Difference between load temperature and ambient temperature at time interval i ($^\circ C$)
\dot{q}	Specific cooker power ($W\ m^{-2}$)	η	Instantaneous efficiency (-)
\dot{q}_0	Specific cooker power for $\Delta T_{f,a} = 0\ ^\circ C$ ($W\ m^{-2}$)	$\eta_{exp,i}$	Efficiency at time interval i (-)
\dot{q}_{Tf}	Specific cooker power when load temperature is T_f ($W\ m^{-2}$)	η_0	Efficiency at $\chi = 0$ (-)
R^2	Coefficient of determination (-)	Subscripts	
s	Slope related variable of the regression expressed by Eq. (2) ($W\ m^{-2}\ ^\circ C^{-1}$)	n	Direction normal to beam radiation
s_Q	Slope related variable of the regression expressed by Eq. (3) ($W\ ^\circ C^{-1}$)	i	Time interval i
s_q	Slope related variable of the regression expressed by Eq. (4) ($W\ m^{-2}\ ^\circ C^{-1}$)	Abbreviations	
T_a	Ambient temperature ($^\circ C$)	SC60	Solar funnel cooker with 60 % of the reflective surface area of design SC100
\bar{T}_a	Average ambient temperature during a test ($^\circ C$)	SC70	Solar funnel cooker with 70 % of the reflective surface area of design SC100
T_f	Load temperature ($^\circ C$)	SC80	Solar funnel cooker with 80 % of the reflective surface area of design SC100
$T_{f,max}$	Maximum value of load temperature ($^\circ C$)	SC90	Solar funnel cooker with 90 % of the reflective surface area of design SC100
$T_{f,i}$	Initial load temperature of a certain time period ($^\circ C$)	SC100	Solar funnel cooker reference design
$T_{f,f}$	Final load temperature of a certain time period ($^\circ C$)		

For instance, the HotPot solar cooker has an interesting design of a foldable reflector made of aluminium, and it incorporates a specific design of cooking vessel with glass enclosure to ensure a greenhouse effect around the black cooking pot [6]. A new version of the funnel cooker made with reflective plates of composite material has been experimentally tested in Malaga-Spain [7–9] and also studied through ray-tracing simulation [10]. According to the experimental results of tests performed by Apaolaza-Pagoaga et al. [9], the values of maximum achievable load temperature were 125.4 $^\circ C$ and 154.5 $^\circ C$, when the funnel cooker was tested without and with a glass transparent enclosure, respectively.

Ruivo et al. [7] also performed experimental work to determine the standardised power values of a funnel cooker, operating under low sun elevation, with a massive glass enclosure around a black enamelled steel pot when either a glass lid or a metal lid is used. The experiments were conducted with a load ratio of 4 kg of water per m^2 of maximum collecting area.

It was found that when a glass lid is used, the standardised power value is 46 % greater than the value obtained when a black lid is used. In another study, Apaolaza-Pagoaga et al. [8] tested several funnel cookers with the same reflector side-by-side but adopting trivets of variable height to support the cooking set. The authors found that the variation in the cooking power due to changes in trivet height is low, and for this reason, it was not possible to be estimated accurately with the procedure

reported in the ASAE S580.1 Standard [11].

Several designs of solar cookers with similar aperture area were tested following the ASAE S580.1 Standard [11], and the corresponding test reports are available online [12]. It is important to point out that the values of standardised power of the different cookers, usually reported by most of testers, were derived from experiments where only a single cooker was tested. Thus, the sun elevation angle range during the test of one solar cooker can be strongly different from the test of another solar cooker, causing a varying impact on the performance parameters of most of the cooker designs tested.

Ebersviller and Jetter [13] tested at the same time a parabolic solar cooker, a box solar cooker and the HotPot solar cooker. The authors found that, in the case of the HotPot solar cooker, the amount of evaporated water was around 6.9 % of the initial amount of water loaded inside the pot. This fraction of evaporated water, even though relatively small, causes an error in calculating the power values when using the formula recommended by the ASAE S580.1 [11]. The formula is strictly valid for a heating water test with negligible evaporation. Thus, neglecting the water evaporation in the last part of the heating test is expected to cause an underestimation of the standardised cooking power.

The ASAE S580.1 Standard [11] establishes the minimum and the maximum values of solar irradiance, ambient temperature and wind velocity to ensure that the obtained results of one or more tests are valid.

Table 1

Panel solar cookers performance data.

Cooker design	Maximum aperture area (m ²)	Standardised power (W)	Efficiency (-)
Hotpot [13]	0.287	25	0.12
Regattieri [15]	0.720	83	0.16
CooKit [12]	0.467	58	0.18
Haines 1 [12]	0.307	41	0.19
Haines 2 [12]	0.500	82	0.23
Funnel cooker [8]	0.500	82.3	0.23
COP Ninety [16]	0.238	29.8	0.18
COP Flower [16]	0.197	17.4	0.13
COP Cave [16]	0.174	15.4	0.13

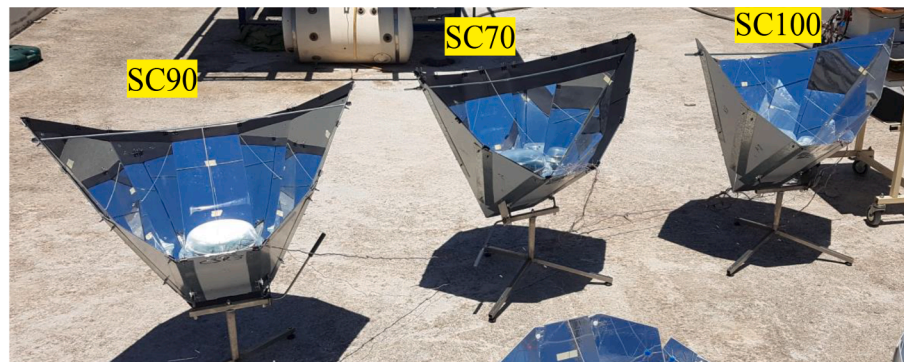
However, when a minor change in a cooker design is being investigated, the difference in the standardised power values cannot be predicted accurately by the procedure indicated in the Standard [11]. Moreover, the Standard also establishes that a solar cooker should be tested using a fixed amount of load. Thus, in procedure of the Standard it is not strictly suitable to investigate the impact of different amounts of the load on the performance of cookers. Moreover, when investigating a minor change in the cooker design, it is very important to carry out experiments by testing two or more cookers with minor design changes at exactly the same time. By following this experimental approach, the uncontrolled weather variables affect the performance of each cooker being tested in the same way. When tests are conducted on different days or in different locations under different conditions, the comparison of performance results of different cookers is not objective.

Designs of several cookers are typically the product of empirical trial and error. A variety of factors are considered: ease of construction, handling, wind resistance, cost, durability, thermal performance, etc. Panel solar cookers, with or without a funnel shape, have in general a small aperture area, i.e., a value less than 0.5 m² [5]. This small size is convenient when cooking for one to three individuals. Logically, using a

solar cooker with a larger aperture area, is expected to result in a more powerful device, but such an increasing in power of the cooker can be small due to a strongly reduction on its optical efficiency when a high number of photons are not intercepted by the receiver. Moreover, very large cookers are not ergonomic in practical use for most solar cooking end-users. A small sized funnel cooker might be convenient in terms of portability, the low space required for its operation and its ability to cook successfully under real-world conditions.

It is essential that the food being cooked reaches the pasteurisation temperature in a short period of time to avoid the risk of bacteria developing. Besides this, water should reach its boiling point soon (for example, making a soup), and for frying, the oil must reach the right frying temperature within a practical time period. Most of the commonly available panel solar cookers are capable of making soup on a clear sky day, however, even for them, the normal frying process is almost impossible.

Chepkurui and Biira [14] carried out tests of funnel solar cookers, constructed with plates of common cardboard, with different four sizes. The experiments were conducted simultaneously by using similar black pots in each cooker. The maximum achievable load temperature values



a)



b)

Fig. 1. Experimental set-up of testing three funnel solar cookers side-by-side: a) cookers SC90, SC70 and SC100 and b) SC100, SC60 and SC80, c) weather station near the cookers being tested and d) weather station located upon the school building.



c)



d)

Fig. 1. (continued).

were relatively low, below the boiling point of water at sea level, and normally recommended heat traps were not used. The four funnel cookers were relatively small, and the aperture area of each size was not provided by Chepkurui and Biira [14].

Table 1 summarizes the maximum aperture area and the standardised power of different designs of solar cookers tested with water. It is important to point out that these listed values of the standardised power

values were derived for the instant when the load is at a temperature of 50 °C greater than the ambient temperature [11]. As briefly mentioned in section 3. Procedure for evaluating the cooker performance parameters, the procedure of the Standard [11] overestimates the standardised power of a cooker. The efficiency listed in Table 1 corresponds to the ratio between the standardized power value, when the load temperature is 50 °C higher than the ambient temperature, and the energy rate

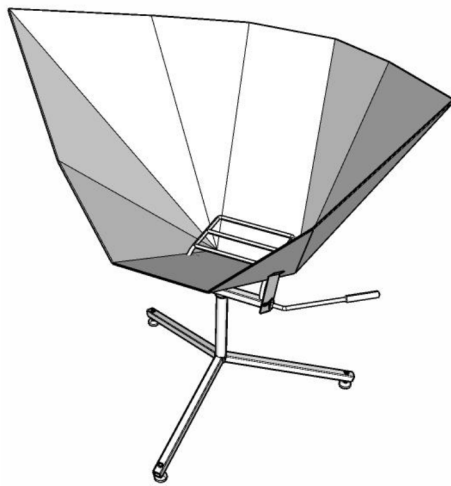


Fig. 2. Funnel solar cooker.

associated with the incoming solar radiation, for a solar irradiance of 700 W m^{-2} , in an area equal to the maximum aperture area of the cooker.

According to the authors, the investigation of the performance of a funnel cooker with different aperture areas has not been formally analysed and quantified by other researchers, and it is not available in scientific literature. Such aspects have not been investigated even for other types of solar cookers. In the case of funnel cookers, it is very important to perform this kind of investigation to optimise the size of the reflector according to a fixed size of the cooking vessel. In this regard, the research carried out by Chepkurui and Biira [14] with different funnel cookers could have been even more useful if cookers were tested with heat trap devices.

Thus, coming back to the current project, this work quantifies the impact of reducing the aperture area of a funnel cooker on its performance and its ability to cook successfully. Outdoor experiments were conducted at high sun elevation angles, with glycerine as the load material, to investigate the impact of the aperture area of a funnel cooker. Glycerine was used on accounts of its capacity for having a load temperature range larger than that available for water. Three cookers were tested at the same time to evaluate the impact on their performance when the aperture area changes. The determined dependences of the cooker opto-thermal ratio and the reference time on the aperture area were used to predict how the solar irradiance impacts on i) the maximum temperature achieved by the load, ii) the time duration required for achieving specific values of the load temperature, and iii) the power of the cooker. At the end of section 5, a brief discussion of the exploratory results on testing solar funnel cookers with different aperture areas is presented. In addition, a comparison of the performance of the funnel cookers tested in the current study, with the performance of a different design of solar cooker recently tested in another research, also with glycerine, is shown. Based on the opinion of the authors, the current study should be continued by carrying out tests of the proposed funnel cooker design with extended reflectors. The authors are confident that this kind of study, not yet published, has an important scientific value that probably will likely push other research teams to perform similar experiments with other cooker designs.

Experimental set-up for testing solar cookers

The experimental set-up used in previous investigations [8,9] was also adopted in the current work to test a set of three solar cookers at the same time as illustrated in Fig. 1. The reflector of each cooker is made of polished aluminium, set over a tripod as shown in Fig. 2. Each cooker has a trivet fixed to the upper part of the tripod. The device illustrated in

Table 2

Reflector geometrical data of the five cookers tested.

Cooker design	SC60	SC70	SC80	SC90	SC100
l_p (m)	0.461	0.506	0.547	0.586	0.623
w_p (m)	0.230	0.230	0.230	0.230	0.230
w_c (m)	0.162	0.117	0.76	0.37	0
$A_{n,max}$ (m ²)	0.307	0.356	0.404	0.452	0.5
A_{ref} (m ²)	0.638	0.744	0.850	0.957	1.063



Fig. 3. Location of temperature sensors used for measuring glycerine temperature.

Fig. 2 corresponds to the reference cooker version here named SC100, the cooker located on the right side of Fig. 1a). This funnel solar cooker has an aperture area, i.e., an effective maximum solar radiation collecting area of 0.50 m^2 . Strips of thin black cardboard were attached to the edges of the reflector to reduce the total area exposed to the sun for the other versions. SC90, SC80, SC70 and SC60 cookers had reflective surface areas of 90 %, 80 %, 70 % and 60 % of the total reflector area of the SC100 solar cooker, respectively.

As described in previous work of Ruivo et al. [7], and also in Chepkurui and Biira [15], each funnel reflector can be constructed by using two rectangular plates. Even the differences between the funnel cooker designs adopted in the previous studies of Ruivo et al. [7] and Chepkurui and Biira [15], both studies' funnel cooker designs can be constructed starting with two rectangular plates. Each plate is defined by a square part, with a side length of l_p , and a rectangular part, with a width of w_p and with the same length l_p . In the context of the current work, the variable l_p represents the effective side length of the square part and the effective length of rectangular part of the reflector plate. These dimensions of the plates are listed in Table 2 for all cookers tested in the scope of the current work. The strip width (w_c), the effective reflector area (A_{ref}), and the effective maximum solar radiation collecting area ($A_{n,max}$) for each design are also indicated in Table 2. In the particular case of the experiments shown in Fig. 1a), the SC100 design appears in the right side, while SC90 and SC70 appear in the left side. In the case of Fig. 1b), the SC100 design appears in the left side, while SC60 and SC80 appear in the right side. The two pyranometers used near the location of cookers for measuring the global solar irradiance are shown in Fig. 1b) and 1c). Fig. 1d) shows the sensors of the weather station located upon the school building.

Similar cooking vessels composed of a black enamelled steel pot and a glass enclosure were used when testing the three cookers simultaneously. Each pot weighed 0.540 kg and had a maximum capacity of three litres, while its glass lid weighed 0.366 kg . Each pot and the respective lid were placed inside a transparent glass enclosure, which

Table 3
Data of the instruments.

Equipment	Model	Variable measured	Operation range	Technical specifications
Thermometers	Thermocouple type T (TC Ltd.)	Temperature of glycerine (°C)	−75 to 250	Tolerance value: ± 1.0 °C
Thermometer	Thermistor S-TMB-M002 (Hobo Onset)	Ambient temperature (°C)	−40 to 75	Accuracy < ± 0.2 °C from 0 to 50 °C
Anemometer	3 cup anemometer S-WSB-M003 (Hobo Onset)	Air speed (m s ^{−1})	0 to 76	Accuracy: $\pm 4\%$ of reading whichever is greater Resolution: 0.5 m s^{-1}
Pyranometer	LP02 (Hukseflux)	Global solar irradiance (W m ^{−2})	0 to 2000	Calibration uncertainty < 1.8 %
Pyranometer	LP02 (Hukseflux)	Global solar irradiance (W m ^{−2})	0 to 2000	Calibration uncertainty < 1.8 %
Pyranometer	CM 21 (Kipp & Zonen)	Global solar irradiance (W m ^{−2})	0 to 4000	Accuracy expected maximum errors: 2 %
Pyranometer	SPN1 (Delta-T Devices Ltd)	Diffuse solar irradiance (W m ^{−2})	0 to 2000	Overall accuracy: $\pm 8\% \pm 10 \text{ W m}^{-2}$

weighed approximately 2.100 kg.

Thermocouples type T were used to measure the temperature of glycerine in five positions as depicted in Fig. 3. All the thermocouples were set at 10 mm from the bottom of the pot. One thermocouple was kept in the central position and the other four sensors formed a square whose vertices were all approximately 10 mm from the pot wall. Each sensor was attached to the vertical part of the corresponding thin L-shaped stainless-steel rod. Each rod was fixed by its horizontal part to the bottom of the pot. The total mass of the rods and the thermocouple cables is negligible.

The average temperature measurements performed by different sensors in each pot was assumed to be equal to the average temperature of glycerine, a value that was used to calculate the power of the cooker.

The wind speed and the ambient temperature were measured, respectively, by an anemometer and a thermometer of the weather station shown in Fig. 1c). The measured values were logged every sixty seconds instead of every 10 min as recommended by the ASAE S580.1 Standard [11].

The global solar irradiance on the plane normal to the beam solar radiation was not directly measured by a pyranometer. Similar to previously published works [8–10], it was computed through the Liu-Jordan isotropic sky model [17] by using data measured by one pyranometer placed in a horizontal plane and another pyranometer placed in a tilted plane making an angle of 50° with the horizontal plane as shown in both Fig. 1b) and 1c). Both pyranometers were azimuthally adjusted every 20 min.

The diffuse fraction of global horizontal radiation obtained from measurements of solar irradiance, given by a SPN1 Sunshine Delta-T Devices Pyranometer located in another nearby meteorological station shown in Fig. 1d), and albedo of 0.2 were considered in the procedure of calculation the global solar irradiance on the plane perpendicular to the beam radiation. This global solar irradiance on the plane normal to the beam solar radiation could be measured alternatively by only a pyranometer if a continuous sun tracking system with both tilt and azimuth adjustments was adopted.

The solar irradiance measured by the pyranometers, and the temperature measured by the thermocouples inside the pot, were logged

every fifteen seconds. The mean value of both variables was calculated every sixty seconds in order to perform subsequent calculations.

The experiments were conducted at the University of Malaga, Spain, a place with a latitude of 36.9°N, between 29th June 2021 and 13th July 2021. In the case of this set of experiments, the solar cookers being tested tracked the sun, azimuthally and also accordingly to the sun elevation angle, by manual operation every 20 min, but both pyranometers located nearby the cookers were adjusted only azimuthally. Due to the manual tracking operation, each cooker remained static during the mentioned time interval of 20 min, i.e., the cooker at the end of each time interval was not perfect aligned to the sun, the maximum deviation in azimuth being about 5°. The maximum deviation for the height of sun, during each experiment, depended on the changes on the sun elevation, but it was estimated to be smaller than 4°. Moreover, the optical efficiency of the funnel solar cooker tested by Carrillo-Andrés et al. [10] was estimated to be above 95 % for a tracking period of 20 min.

All the measured data was automatically logged in specific data loggers: i) Hobo Weather Station data logger, for the local weather station, where ambient temperature and wind speed are measured, ii) Campbell Scientific CR1000 data logger with an AM16/32B Multiplexer, where the load temperature was measured by the thermocouples located inside each pot and global solar irradiance was measured by the two pyranometers located near the solar cookers being tested and iii) Campbell Scientific CR1000 data logger located in the school's weather station, about 6 m vertically above and about 10 m away of the solar cookers testing area, where the global horizontal solar irradiance, diffuse horizontal solar irradiance, air humidity and ambient temperature, wind speed were measured. The obtained recorded files at the end of each experiment were transferred to a computer. In the case of the current study, the measured data was used to calculate the several performance parameters and to plot graphs.

Table 3 lists data of the instruments used. More details about the measurement systems used in present study can be also found in previous work of the above-mentioned authors [7,9].

Procedure for evaluating the cooker performance parameters

The procedure adopted to conduct the tests and process the experimental data presents important deviations with respect to the procedure indicated in the ASAE S580.1 Standard [11]. The load ratio recommended by the Standard is 7 kg m^{-2} . This relatively high value is not representative of the cooking load being adopted in a real cooking context. The capacity of the pots used by most of solar cooking end-users is not large enough to fulfil this specific recommendation of the Standard. Moreover, pots in real cooking contexts are often used most of the times at partial loads. Thus, in the current work, smaller values of the load ratio were adopted. The Standard proposes a methodology to process the data acquired through the test protocol that requires the use of water as load to determine the standardised power of a solar cooker. In the current work, this procedure is not adopted because the physical meaning associated with the linear regression derived from observations of standardised power values does not represent the performance of a cooker at a solar irradiance of 700 W m^{-2} . The standardised power value reported, when the load is at a temperature of 50 °C greater than the ambient temperature, is overestimated. Thus, linear regressions expressed in terms of cooker power and efficiency are adopted in current work. Moreover, glycerine has been preferred as a test load due to the limitations imposed by the used of water as load. Using glycerine as load, i) enables the investigation of cookers performance at a temperature higher than the water boiling point at common atmospheric pressure values adopted in domestic cooking at sea level and at altitude, ii) allows better insight into the resolution of the thermal performance parameters as its specific heat is lower than that of water, iii) offers a higher resolution in design-induced changes in thermal performance parameters and iv) enables the more realistic determination of thermal performance parameters for a specific design of solar cooker at low and

intermediate-range of temperature [1,4,9].

The rate of the load temperature variation dictates the rate of the thermal energy stored by the load, which is a fraction of energy associated with the incoming solar radiation. Thus, the instantaneous efficiency term η is here adopted to characterize this part of the incoming energy rate that is stored by the load. Knowing the load temperature at two instants, spaced by a time interval, Δt_i , the efficiency can be estimated for each time interval i by:

$$\eta_{\text{exp},i} = \frac{m_f c_f \Delta T_{f,\text{exp},i}}{\Delta t_i I_{n,\text{exp},i} A_{n,\text{max}}}, \quad (1)$$

where the variable $\Delta T_{f,\text{exp},i}$ represents the variation of the load temperature in the time interval i . The global normal solar irradiance $I_{n,\text{exp},i}$ is the average value at the same time interval. Eq. (1) has been used in previous studies of Ruivo et al. [18,19], but not exactly in the same manner. In those previous studies [18,19], i) the average value of the solar irradiance during the test was adopted instead of the value of solar irradiance at each time interval i and ii) the variation of load temperature in each time interval i was estimated from a derived fitted exponential curve instead of using the variation of load temperature measured experimentally.

The parameters c_f and m_f represent the specific heat and mass of the load, respectively.

For each time interval, there is a difference between the average values of load temperature and ambient temperature, which is represented by $\Delta T_{f,a,\text{exp},i}$. The corresponding specific temperature difference $\chi_{\text{exp},i}$ is given by the ratio of $\Delta T_{f,a,\text{exp},i}$ to the solar irradiance $I_{n,\text{exp},i}$.

Plotting the discrete values of the power $\eta_{\text{exp},i}$ as a function of $\chi_{\text{exp},i}$, the performance curve for the efficiency η against the specific temperature difference χ can be determined from a single test or from a set of tests of the same cooker design [18,19]:

$$\eta = \eta_0 - s \times \chi \quad (2)$$

The power of a solar cooker has been defined as the rate of storage of thermal energy by the load [7,8,11,13,14,17,19–21]. Thus, for particular values of the solar irradiance (I_n) and ambient temperature (T_a), the cooker power can be related with efficiency by:

$$\dot{Q} = \eta I_n A_{n,\text{max}} \quad (3)$$

The performance curve expressed by Eq. (2) can be used to derive the linear curve of power [18]:

$$\dot{Q} = \dot{Q}_0 - s_Q \Delta T_{f,a} \quad (4)$$

or the linear curve of the specific cooker power ($\dot{q} = \dot{Q}/A_{n,\text{max}}$).

$$\dot{q} = \dot{q}_0 - s_q \Delta T_{f,a} \quad (5)$$

where $\Delta T_{f,a}$ is the difference between load temperature and ambient temperature. The parameters s_Q and s_q are the slope related variables of the linear regressions expressed by Eqs. (4) and (5), respectively. The parameters \dot{Q}_0 and \dot{q}_0 are, respectively, the cooker power and the specific power that correspond to the point of no thermal losses from the load to the ambient and to the surroundings, i.e., when $\Delta T_{f,a} = 0^\circ\text{C}$. The following relations between the parameters of the three linear curves can be written:

$$\dot{Q}_0 = \eta_0 I_n A_{n,\text{max}} \quad (6)$$

$$\dot{q}_0 = \eta_0 I_n \quad (7)$$

$$s_Q = s \times A_{n,\text{max}} \quad (8)$$

$$s_q = s \quad (9)$$

In the current work, glycerine was heated up to a very high temperature where the rate of its temperature variation was small. Thus, it is

important to select a set of observation points well distributed in the whole range of temperature to determine the linear performance curves instead of a regular distribution of points. So, observation points spaced at least by a variation $\Delta T_{f,\text{exp},i}$ of 2°C in the load temperature were selected, but at the initial heating period points with a temperature difference $\Delta T_{f,a,\text{exp},i}$ smaller than 20°C were not taken into account.

It can be demonstrated that the ratio \dot{Q}_0/s_Q corresponds to the temperature difference $\Delta T_{f,a}$ used in Eq. (4) when $\dot{Q} = 0$ W, which is here named $\Delta T_{f,a,\text{max}}$. This point of the performance curve given by Eq. (4) corresponds to the point with $\eta = 0$ in the performance curve expressed by Eq. (2), where $\chi = \chi_{\text{max}}$. By following the formulation of Ruivo et al. [18], the value of the cooker opto-thermal ratio COR corresponds to the value of χ_{max} and the cooker reference time corresponds to:

$$t_{\text{ref}} = \frac{m_f c_f COR}{\eta_0 A_{n,\text{max}}} \quad (10)$$

Knowing both the parameters, the performance of the cooker can be predicted for constant conditions of solar irradiance I_n and ambient temperature T_a , but for the amount of the same fluid adopted as load and cooking vessel equal to those used in the derivation of the regression expressed by Eq. (2). Regarding the maximum theoretical achievable load temperature, it can be estimated by [18]:

$$T_{f,\text{max}} = T_a + I_n COR \quad (11)$$

The theoretical time period, $t_{i,f}$, required for heating up the load from the initial temperature $T_{f,i}$ to a particular value of temperature $T_{f,f}$, in a process without phase change and with the initial load temperature equal to the ambient temperature, can be estimated by [18]:

$$t_{i,f} = t_{\text{ref}} \ln \left(\frac{\frac{T_{f,i} - T_a}{I_n} - COR}{\frac{T_{f,f} - T_a}{I_n} - COR} \right) \quad (12)$$

The power of the cooker, at the instant when the load temperature is T_i , can be predicted by [18]:

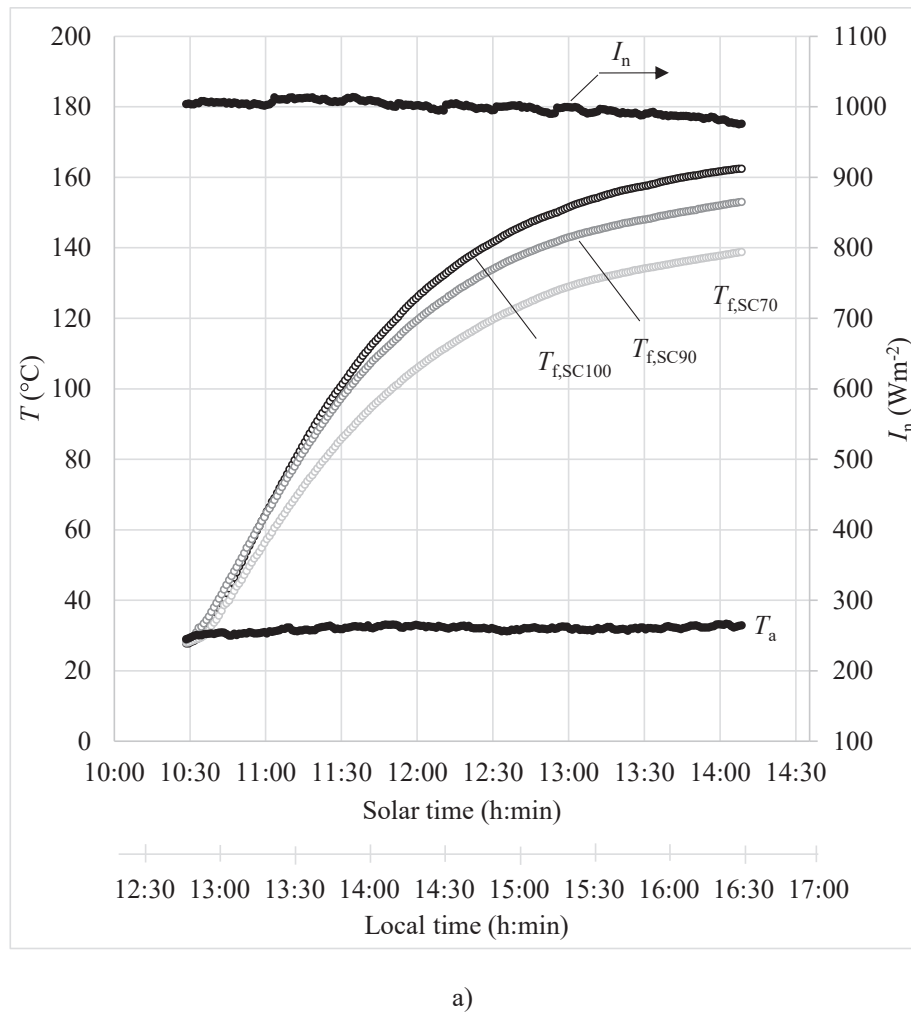
$$\dot{Q}_{Tf} = - \frac{m_f c_f}{t_{\text{ref}}} (T_i - T_a - I_n COR) \quad (13)$$

for the load heating with the same mass of value m_f and taking place under constant values of I_n and T_a . Similarly, the specific power of the cooker is:

$$\dot{q}_{Tf} = - \frac{m_f c_f}{t_{\text{ref}} A_{n,\text{max}}} (T_i - T_a - I_n COR) \quad (14)$$

These two Eqs. (13) and (14) are equivalent to Eqs. (4) and (5), respectively.

It is important to point out that procedure of obtaining the COR parameter is not strictly equal to the procedure that has been adopted in most of the previous published studies [1–5]. In these studies, the experimental measured temperature of the load during its heating process was fitted by an exponential regression curve that was then used to derive a linear regression performance curve, which was used to determine the COR and also other parameters. In the current study, this linear regression is obtained directly from the discrete points associated with the discrete values of efficiency calculated by Eq. (1) and $\Delta T_{f,\text{exp},i}$. In the case of an ideal test conducted under constant solar irradiance and constant ambient temperature, both the approaches provided same linear regression curve and thus the same COR . Real tests must be considered valid when the variations of solar irradiance and ambient temperature are small, i.e., when the average values of solar irradiance and ambient temperature well represent the behaviour of these two parameters during each experiment. Under these conditions, the difference between the values of COR obtained by both approaches is expected to be small. It is also important to point out that, in the current



a)

Fig. 4. Plots of global solar irradiance, ambient and glycerine temperature measured during: a) the Expt. no. E141A and b) the Expt. no. E145A.

work, the ratio of the thermal capacitance of the load per unit of aperture area adopted in testing the different cookers with different aperture area is not equal to $10.46 \text{ kJ } ^\circ\text{C}^{-1} \text{ m}^{-2}$, a value that has been adopted in previous studies and known as standard value. This standard value was not followed in the current work because the mass of the load was kept constant in all test cookers designs. This is an approach that, according to the knowledge and opinion of the authors, was never followed previously and is valid in a scientific investigation about performance of solar cookers.

Evaluation of performance parameters from testing results

In the current study, tests were carried out with 1.736 kg of glycerine loaded inside each pot. The difference between mass of glycerine inside the pot at end and before starting a test was negligible. In the calculations, the specific heat of glycerine was assumed constant and equal to $3014 \text{ J kg}^{-1} ^\circ\text{C}^{-1}$. This assumption has been adopted in previous studies [1–4,9,18,19]. According to the work of Sagade et al. [1], the error is estimate to be less than $\pm 4.4 \%$ in a large range of temperature. The load ratio in the largest and smallest cooker were, respectively, 3.472 kg m^{-2} and 5.655 kg m^{-2} .

Two sets of experiments with three cookers having different aperture area values were performed. The first set (SetA) includes the configurations SC100, SC70 and SC90, while the second set (SetB) includes the configurations SC100, SC60 and SC80.

All measured variables were plotted in time series format. For example, Fig. 4 depicts the plots of the global normal solar irradiance I_n , i.e., the global solar irradiance on the plane normal to beam radiation and also includes the plots of ambient temperature and glycerine temperature of the cookers tested in two different experiments. Fig. 4a) applies to the tests of SC100, SC90 and SC70 solar cookers conducted in the experiment no. E141A performed on 29th June 2021 and Fig. 4b) the tests of the cookers SC100, SC80 and SC60 during the experiment no. E145A performed on 12th July 2021. The solar noon time at the location in this testing day corresponds approximately to 14 h 20 min of local time. The experiment no. E141A started 1 h 31 min before solar noon time and ended 2 h 09 min after solar noon time. The experiment no. E145A started 1 h 03 min before solar noon time and ended 3 h 37 min after solar noon time.

Several tests were carried out during six days to investigate the impact of each cooker design on the respective performance for operation under high sun elevation. Some of the main data of the conducted tests is provided in tables reported in Appendix A. The load thermal capacitance values adopted in the experiments are smaller than the value associated with the load ratio of 7 kg m^{-2} recommended by the Standard, when water is adopted as load [11]. Thus, it is important to verify if the time step of 10 min recommended by the Standard provides good estimations for the efficiency values of the observation points used to derive the linear regression. For this purpose, preliminary calculations with a time steps of 4 min and 10 min were performed to estimate

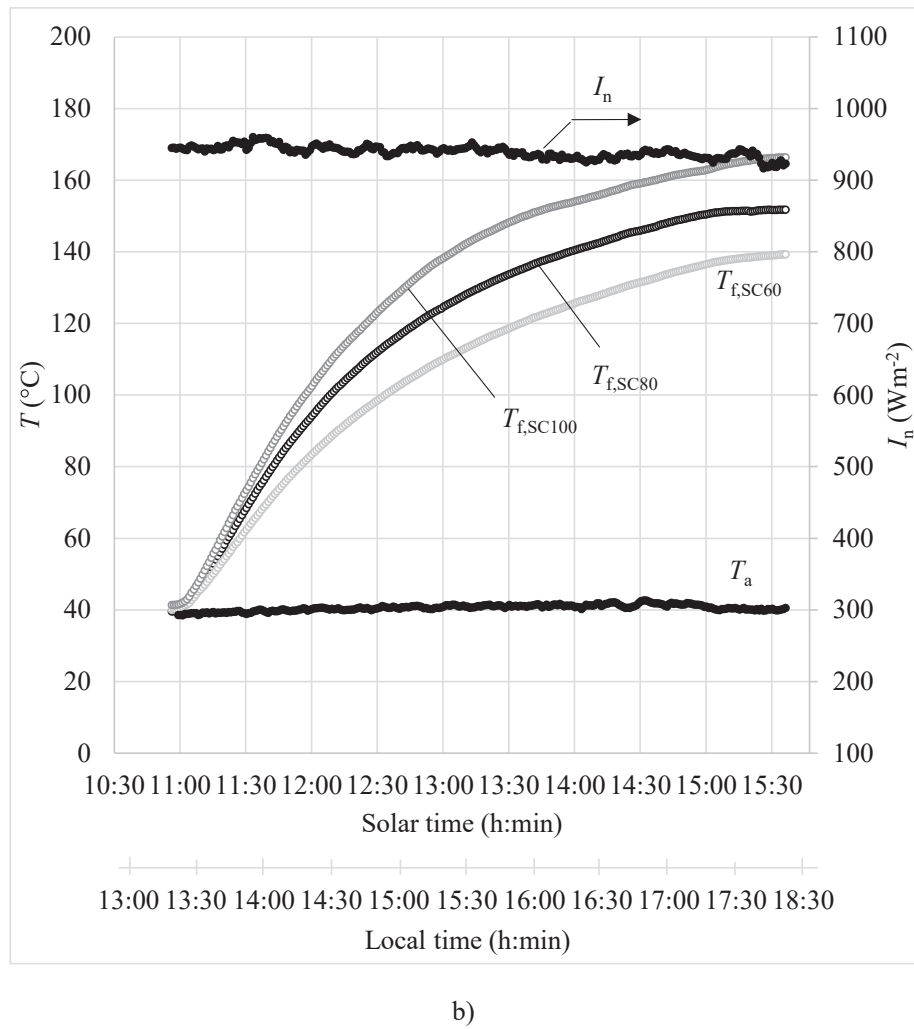


Fig. 4. (continued).

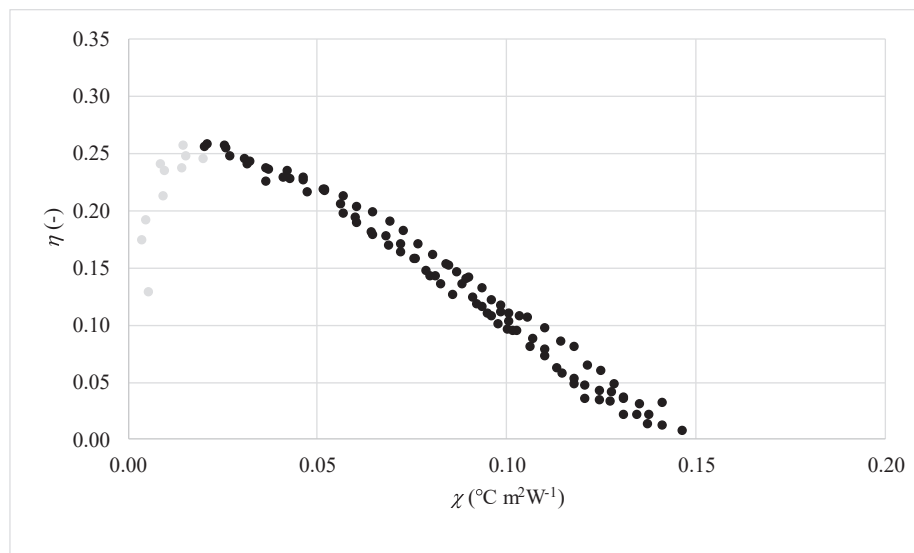


Fig. 5. Plot of observation points of tests conducted with cooker SC100 in experiments of SetA (Expts. E141A, E142A and E143A).

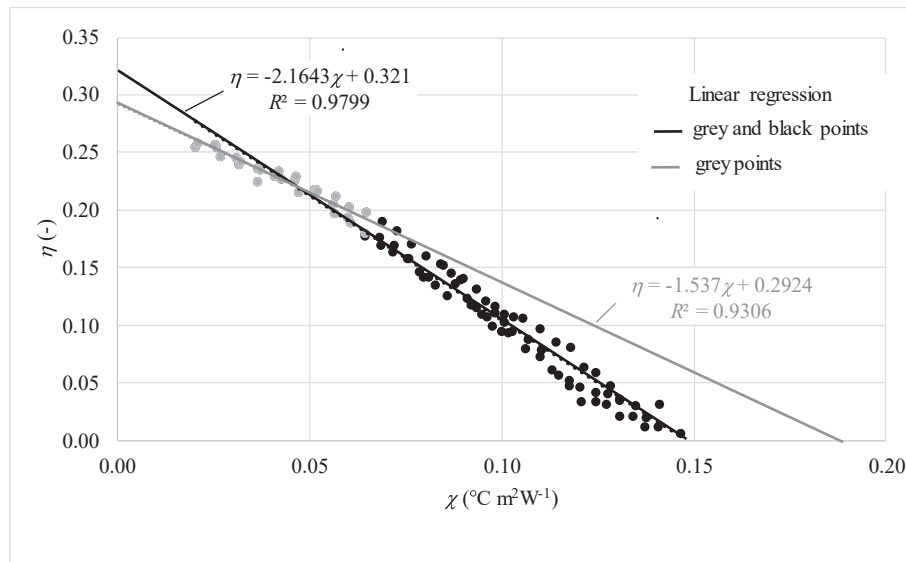


Fig. 6. Linear regressions curves derived from tests conducted with cooker SC100 in experiments of SetA for two ranges of load temperature.

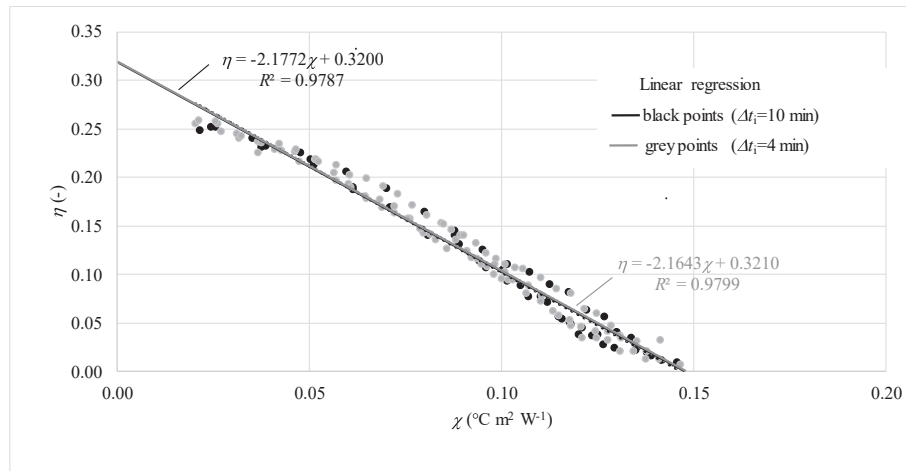


Fig. 7. Linear regressions derived from tests conducted with cooker SC100 in experiments of SetA with time intervals of 4 and 10 min.

the linear regression curve. It is also important to check the differences between the performance curves derived with selected observation points of the whole load temperature range and for the load temperature range recommended by the Standard when water is adopted as load. In this case, the maximum temperature of the load is 95 °C, i.e., 5 °C less than the boiling water point at sea level conditions. Fig. 5 shows the plot of observation points for the efficiency for each time interval of 4 min using the measured data of a set of three tests of the cooker with the largest aperture area, i.e., SC100. The points represented by grey marks clearly show that the efficiency at the beginning of the heating of the load has not a linear decreasing dependence on χ , a behaviour that cannot be detected when plotting observation points calculated with a time interval of 10 min. This evidence shows that the linear regression should be used with some caution [18]. For this purpose, the set of points represented by black marks was selected for the calculation of the linear regression. This set of point is defined by points with $\Delta T_{f,a} > 20$ °C, i.e., values of χ greater than, approximately, 0.02 °C m² W⁻¹.

Fig. 6 shows two sets of observation points obtained with a time step of 4 min and the corresponding linear regressions. The points shown by the grey mark correspond to observation points with a load temperature less than 95 °C. This temperature value corresponds to the higher limit of temperature recommended by the ASAE S580.1 Standard [11] when

Table 4

Results of side by side tests of cookers SC70, SC90 and SC100 in experiments of SetA and of cookers SC60, SC80 and SC100 in experiments of SetB.

Experiments	SetA			SetB		
	E141A	E142A	E143A	E144A	E145A	E146A
Cooker design	SC70	SC90	SC100	SC60	SC80	SC100
n_p	48	49	50	50	52	52
η_0 (-)	0.3516	0.3266	0.3196	0.3368	0.3384	0.3052
$s(W\ m^{-2}\ ^\circ C^{-1})$	2.8933	2.4072	2.1720	3.1334	2.6882	2.2035
R^2	0.9900	0.9869	0.9787	0.9578	0.9625	0.9776
$COR(m^{-2}\ ^\circ C\ W^{-1})$	0.1215	0.1357	0.1471	0.1075	0.1259	0.1385
$t_{ref}(s)$	5080	4809	4818	5439	4818	4749
$T_{f,max}(^\circ C)$	152.8	166.8	178.2	135.7	153.1	165.1
$\bar{T}_a(W\ m^{-2})$	989.1			948.6		
$\bar{T}_a(^\circ C)$	32.6			33.7		

water is used as load at sea level. The points shown by the black marks represent all the remaining observation points where the temperature of the load is greater than 95 °C. The grey linear regression was derived by using only the observation points represented by grey marks. The black line corresponds to the linear regression derived by all points represented by both the grey and the black marks. It is observed, in this

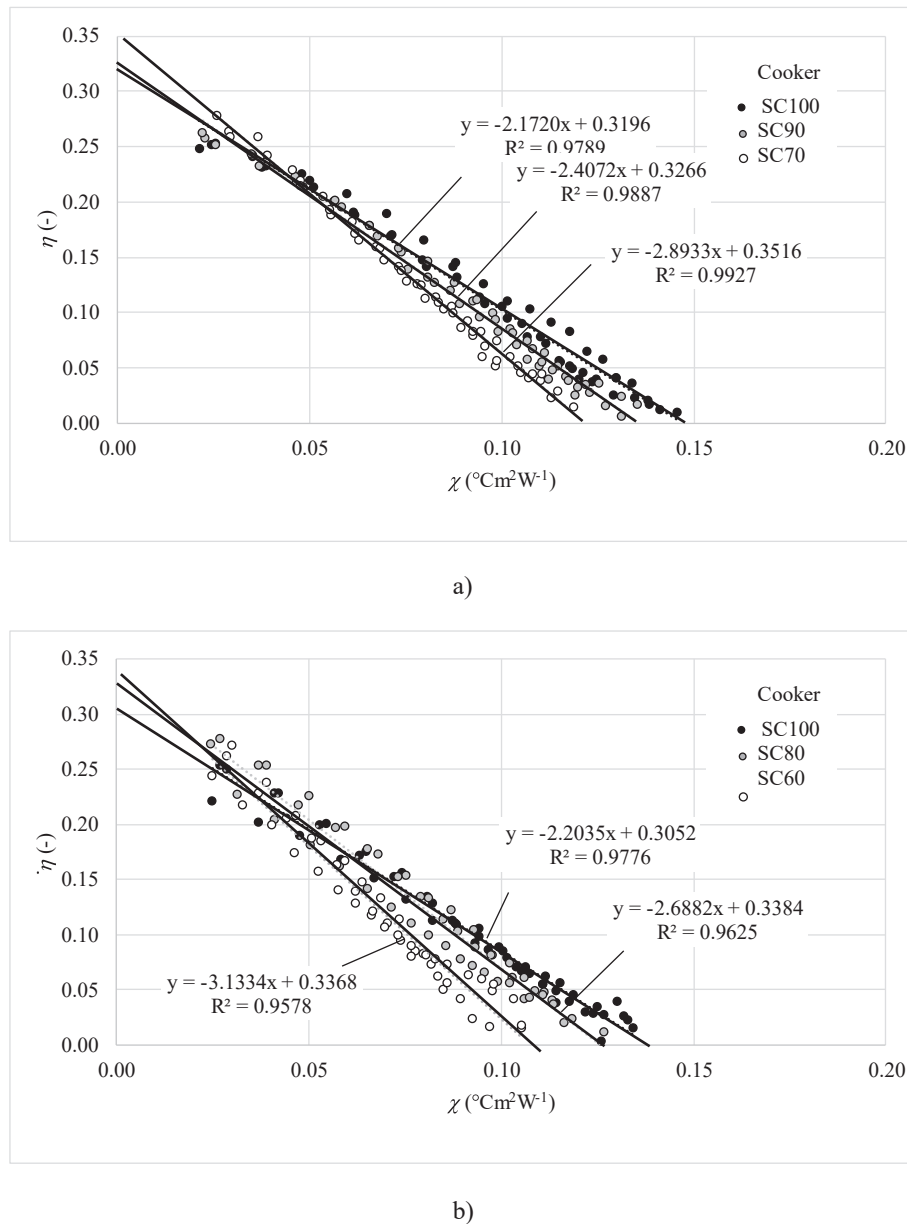


Fig. 8. Linear efficiency regressions derived from: a) tests of SC100, SC90 and SC70 in experiments of SetA and b) tests of SC100, SC80 and SC60 in experiments of SetB.

particular case, that the difference on the values of efficiency estimated by the two linear regressions is equal just in a single middle point, but due to the difference in both slopes, the specific temperature difference χ_{fmax} estimated from the data of the grey line is larger and far from the expected value. For the average conditions of the experiment, $\Delta T_{f,a,max}$ is estimated to be 146.7°C when using the regression derived from all grey and black points, and 190.1°C when using the regression associated with the grey points only. This last estimated value is extremely high and strongly deviates from the value given by the plot of black points depicted in Figs. 5 and 6.

Fig. 7 shows two sets of valid observation points obtained with time steps of 4 min and 10 min. The differences between the shown derived linear regressions are negligible. Thus, a time step of 10 min is adopted in the calculations for the efficiency curve for the reference cooker and also for the other cookers with smaller aperture area.

Table 4 presents the parameters of the derived regression, parameters predicted from the data of the derived regression and the average values of solar irradiance and ambient temperature for the two sets of

experiments SetA and SetB. The COR values obtained for the SC100 cooker from the results of SetA and SetB are, respectively, 0.1471 and $0.1385\text{ m}^2\text{ }^{\circ}\text{C W}^{-1}$. The difference between these two values is relatively low, i.e., it is less than 6 %. It can be justified by some minor deviation to the ideal procedure to carry out the experiments, e.g., minor differences in uncontrollable variables such as intensity and direction of wind. These COR values are smaller than the average value $0.157\text{ m}^2\text{ }^{\circ}\text{C W}^{-1}$ obtained by testing the same cooker under a low sun elevation [9]. This evidence shows that the cooker performance at low sun elevation is better under similar conditions of ambient temperature and solar irradiance. The differences between the average values of the solar irradiance for each experiment are small. Regarding the average ambient temperature, the registered values are relatively high in case of Expts. E143A and E145A (see Appendix A). Fig. 8a) and 8b) depict the observation points and the linear regressions derived from the measured data of experiments of SetA and SetB, respectively. From Fig. 8, it can be observed in both sets of experiments, SetA and SetB, that the cooker configurations with smaller areas have higher instantaneous efficiency

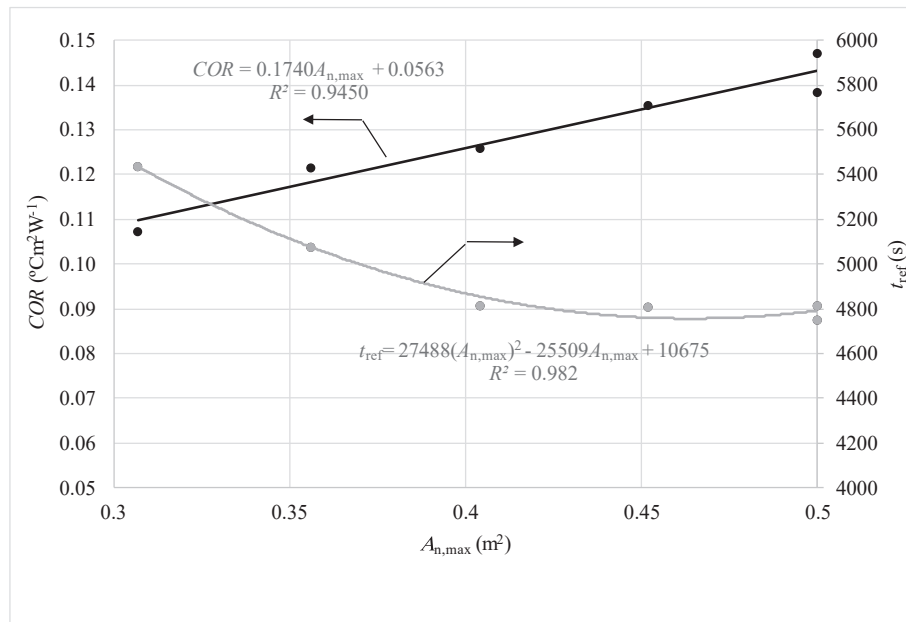


Fig. 9. Influence of cooker aperture area on the cooker opto-thermal ratio and the reference time.

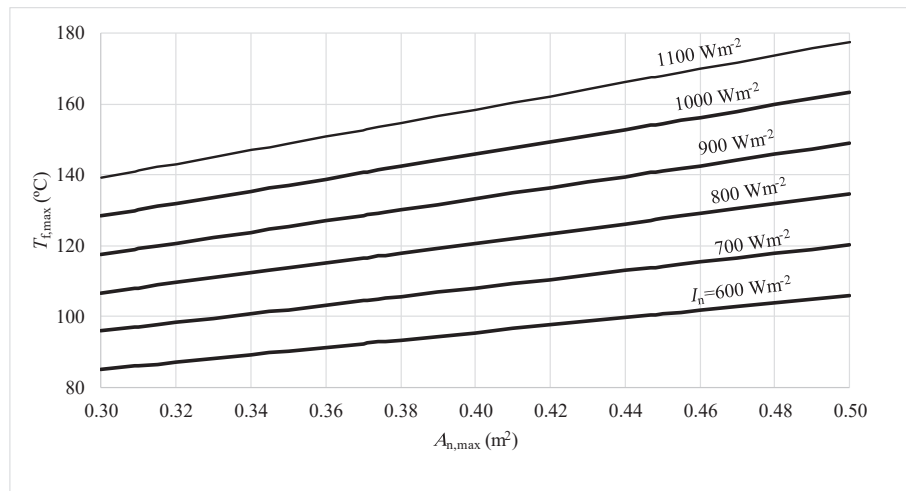


Fig. 10. Influence of cooker aperture area and global solar irradiance on the maximum achievable load temperature.

at the beginning of the heating process of glycerine, but at the end of the heating process, the reference configuration SC100 provides the highest values of χ .

The highest and the smallest values of the maximum load temperature determined from each linear regression for the average ambient temperature and the average global solar irradiance are obtained with the cookers SC100 and SC60, and estimated to be 178.2 °C and 135.7 °C, respectively (Table 4). According to Fig. 4a), the load in the cooker SC100 did not achieve the maximum value in Expt. no. E141A because the test was stopped before achieving the apparent stagnation conditions.

Fig. 9 depicts the plots of COR and t_{ref} as a function of the aperture area, together with the corresponding regression curves.

For an ambient temperature and an initial load temperature equal to 20 °C and a solar irradiance of 700 W m⁻², the highest load temperature provided by the smaller cooker, SC60, for the same mass of glycerine used in the experiments, is estimated with Eq. (11) to be 95.2 °C, which can be seen as a relatively low value and an indicator that cooking success would be questionable. Under these conditions, the time for

taking the load from 20 °C to 90 °C, estimated by Eq. (12), is 4 h 2 min.

Prediction of cookers' performance for different aperture areas and global solar irradiance values

The time period required to cook a specific amount of food and the maximum achievable load temperature are important performance parameters for a solar cooking user. Thus, in the present section, Eqs. (11) and (12) are used to predict the influence of the solar irradiance, in the range of 500 to 1100 W m⁻², and the influence of the cooker aperture area, in the range of 0.3 to 0.5 m², on the parameters $T_{f,max}$ and $t_{i,f}$. In these calculations, the equations of the regressions shown in Fig. 9 are used to estimate COR and $t_{i,f}$ as functions of the cooker aperture area.

Three specific values of theoretical time periods $t_{20,65}$, $t_{20,100}$ and $t_{20,140}$ were considered. The parameter $t_{20,65}$ corresponds to the time required to achieve the batch food pasteurization condition of 65 °C when starting the heating process with load temperature of 20 °C. The parameters $t_{20,100}$ and $t_{20,140}$, instead, correspond to the time required to heat up the load from 20 °C to the water boiling point at sea level and to

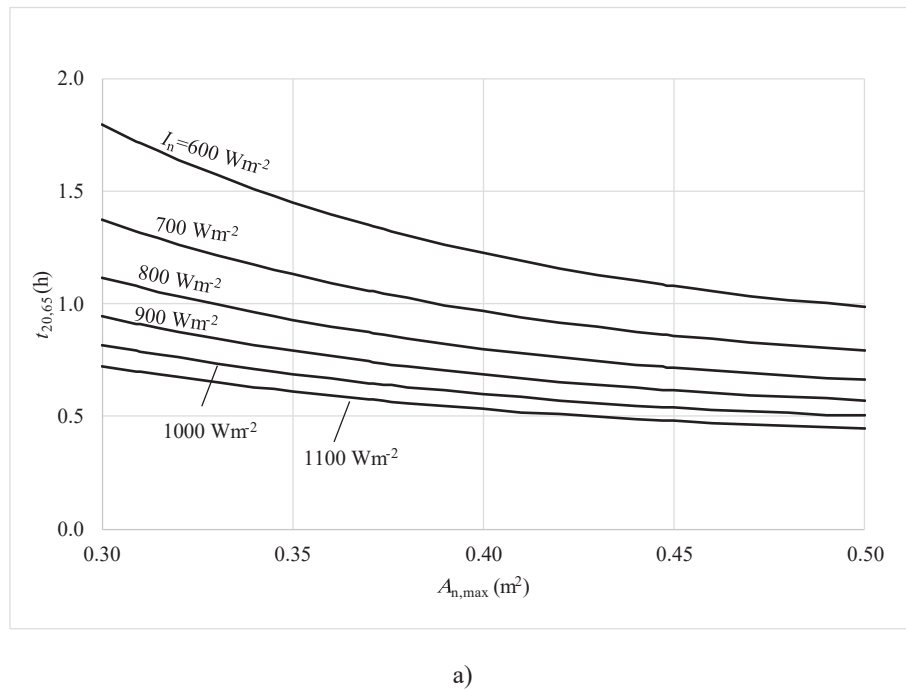


Fig. 11. Influence of cooker aperture area and global solar irradiance on the time parameters: a) $t_{20,65}$, b) $t_{20,100}$ and c) $t_{20,140}$.

an intermediate temperature of 140 °C, respectively.

Also, three specific values of cooker power \dot{Q}_{65} , \dot{Q}_{100} and \dot{Q}_{140} are calculated with Eq. (13) for the instants when load temperature values are 65 °C, 100 °C and 140 °C, respectively. Similarly, the three corresponding values of the specific cooker power \dot{q}_{65} , \dot{q}_{100} and \dot{q}_{140} are calculated with Eq. (13).

Fig. 10 depicts the dependence of $T_{f,max}$ on the global solar irradiance and aperture area when the cooking vessel, load mass and tracking procedure under high sun elevation are those adopted in the experiments. Figs. 11–13 show the influence of the same operating conditions on the time duration $t_{20,65}$, $t_{20,100}$ and $t_{20,140}$, on power values \dot{Q}_{65} , \dot{Q}_{100} and \dot{Q}_{140} and on \dot{q}_{65} , \dot{q}_{100} and \dot{q}_{140} , respectively. It can be seen from Fig. 10, that the pasteurisation temperature of 65 °C is achieved in all investigated conditions. For low solar irradiance and low aperture area, the water boiling temperature is not achieved. For a global solar irradiance greater than 800 W m⁻², the water boiling temperature is achieved independently of the cooker aperture area. The intermediate temperature of 140 °C is achieved independently of the aperture area only for the cases with global solar irradiance greater than 1100 W m⁻². The load temperature $T_{f,max}$ is greater than 100 °C independently of the solar irradiance, only for the highest aperture area, i.e., cooker SC100.

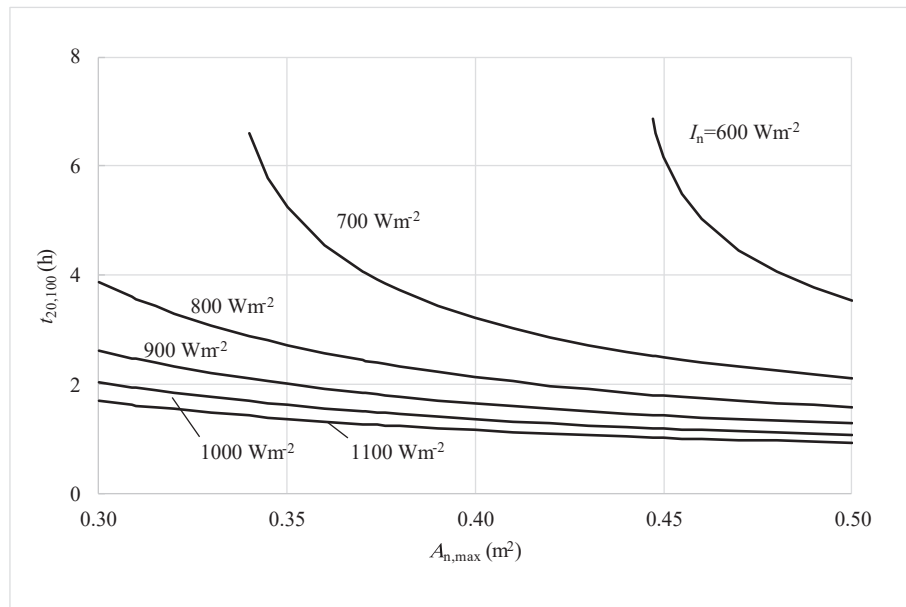
Despite pasteurization temperature being achieved in all simulated cases, it can be observed from Fig. 11 that at relatively low global solar irradiance and for cookers with small aperture area, the time required to achieve the pasteurization temperature is greater than 1 h. As an example, it is 1.79 h in the case of SC60, i.e., a cooker with aperture area of 0.307 m², under a global solar irradiance of 600 W m⁻². On the opposite side, the shortest time of 0.45 h is obtained under an irradiance of 1100 W m⁻² when the cooker SC100 is used. When solar irradiance is greater than 900 W m⁻², it is observed that pasteurization temperature is achieved by all cookers in less than 1 h. Regarding the water boiling temperature of 100 °C, this specific point is reached by all cookers in a period smaller than 2 h if solar irradiance is extremely high. For instance, it is just 0.94 h in the case of the cooker SC100 under a global solar irradiance of 1100 W m⁻². To achieve the intermediate temperature value of 140 °C, the cooker SC100 provides the smallest time of

about 2 h when the solar irradiance is extremely high.

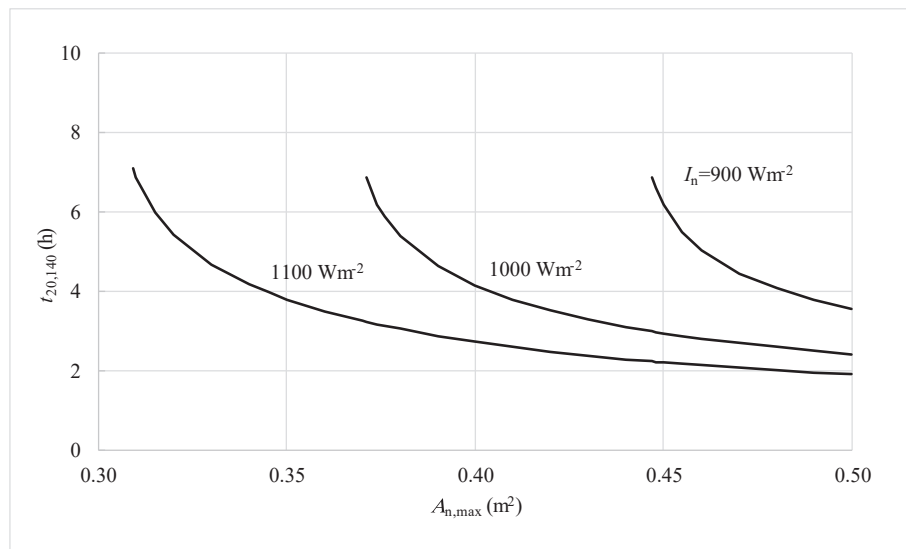
From Fig. 12, it can be seen, as expected, that the power values at pasteurization condition are much higher than the power values at water boiling temperature of 100 °C and at intermediate temperature of 140 °C. As an example, the predicted power at pasteurization temperature under 700 W m⁻² in the cooker configuration SC70 is 38.9 W.

From Fig. 13a), it can be seen that for values of solar irradiance of 1000 W m⁻², the optimum value of the aperture that maximizes the specific cooker power \dot{q}_{65} is about 0.44 m². For a low solar irradiance of 600 W m⁻², the optimum value of the aperture that maximizes the specific cooker power \dot{q}_{65} is about 0.5 m², i.e., the cooker design SC100. It can be also seen that the specific power \dot{q}_{65} of SC100 for higher values of solar irradiance is lower than the value of the optimum area, but the differences are negligible. From the findings of Fig. 13a) and from the observation of Fig. 13b), it can be seen that the optimum area maximizing the specific cooker power \dot{q}_{100} is greater than the aperture area of SC100. The influence of both aperture area and solar irradiance on the efficiency is depicted in Fig. 14 for the instant when the load is at 65 °C. The maximum specific power values clearly observed in Fig. 13a) are justified by the corresponding maximum values of the efficiency shown in Fig. 14.

Chepkurui and Biira [14] made four funnel cookers using plates of carboard and a reflective foil. The designs adopted by Chepkurui and Biira [14] seem to be closer to the conical shape than the funnel cooker designs adopted in the current work because the reflector is composed of more panel elements. Despite these differences, the aperture area of the different versions of funnel cooker made by Chepkurui and Biira [14] are here estimated roughly by assuming that the ratio of the aperture area to the reflector area is similar to the same ratio of the funnel cookers tested in current work. This ratio varies from 0.4704 to 0.4812. Assuming the constant value of 0.475 for this ratio and the dimensions of the cardboard plates provided by the authors [14], the aperture area of the four cookers tested is estimated to range from 0.107 m², in the smallest cooker, to 0.356 m², on the largest cooker. The experiments were conducted with 1 kg of water inside each pot, which dimensions and material are not reported by the authors [14]. Using the published progressions of water temperatures, it can be shown that the power



b)



c)

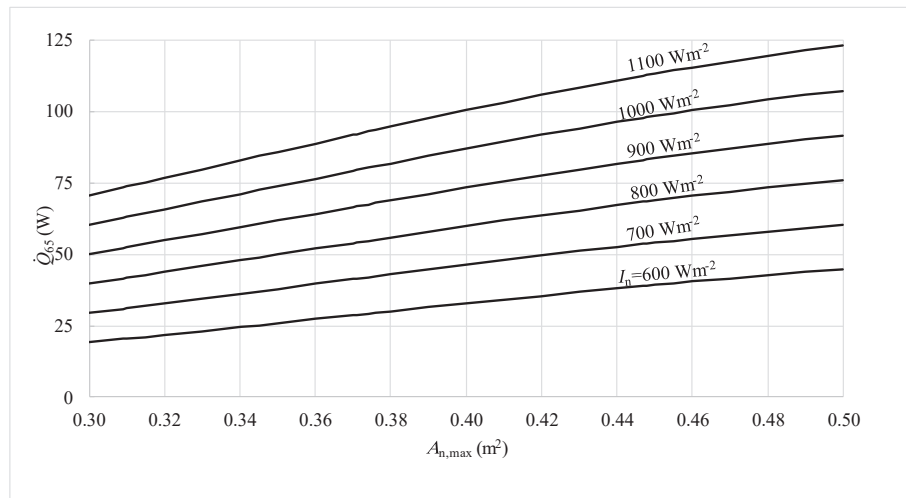
Fig. 11. (continued).

values of the cookers are extremely low when the average solar irradiance over the test period was 684 W m^{-2} . Moreover, in the case of the largest of the cookers, it took about 4 h to raise the temperature of the water by 70°C , which is not a promising result as are the results of other tested cookers listed in Table 1. As example, Apaolaza-Pagoaga et al. [16] tested experimentally different configurations of Copenhagen solar cooker with the same reflector area of 0.542 m^2 , but with different values of the maximum aperture area: 0.174 m^2 for Cave configuration, 0.238 m^2 for Ninety configuration and 0.197 m^2 for Flower configuration. The results of the tests, performed using black pot loaded with 1.5 kg of water [16], were more promising than the results of Chepkurui and Biira [14] because transparent glass enclosures were adopted.

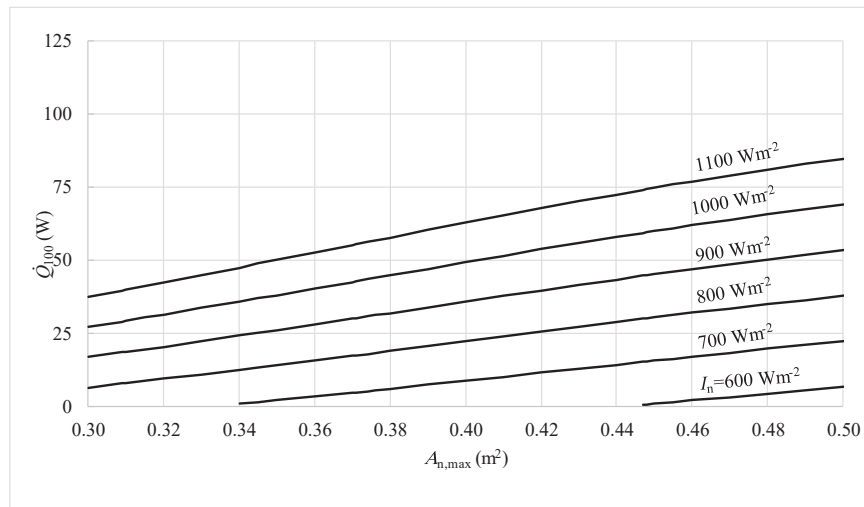
Funnel cookers tested by Chepkurui and Biira [14] and Copenhagen solar cooker tested by Apaolaza-Pagoaga et al. [16] can be categorized as cookers with very small aperture area. Comparing the performance of Copenhagen cooker with larger aperture area (0.238 m^2) with the

performance of funnel cooker with larger aperture area (0.238 m^2) yields that the performance of Copenhagen cooker is much better, mainly to the fact that glass enclosure to heat trap the heat was adopted. In contrast to these small cookers, Coccia et al. [20] have tested a high concentration ratio box solar cooker with multiple reflectors. Some tests were experimentally conducted using peanut oil, ending at a temperature much less than the stagnation point where the heat gain is equal to the thermal losses. The maximum achievable load temperature was estimated by the authors to be around 380°C .

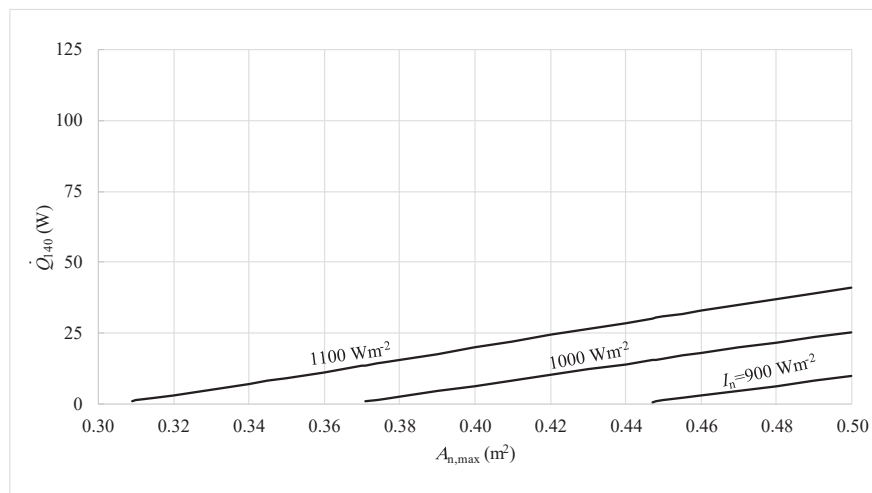
It would be good to compare the influence of cooker aperture area and global solar irradiance on the performance indicators of funnel cookers tested by Chepkurui and Biira [14] with the performance indicators of funnel cookers tested in the scope of current work. For doing such analysis, more details about the tests and cookers tested should be known. Nevertheless, due to the relatively low values of the maximum achievable load temperature obtained by the authors [14], the



a)

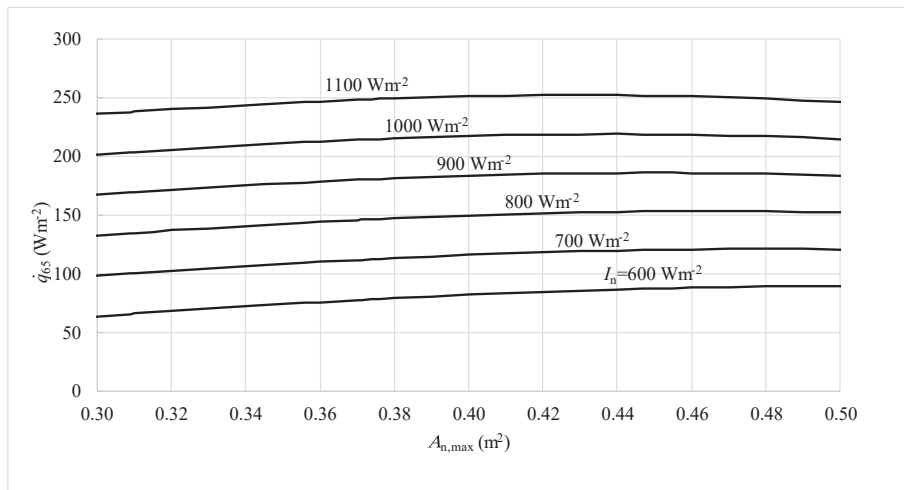


b)

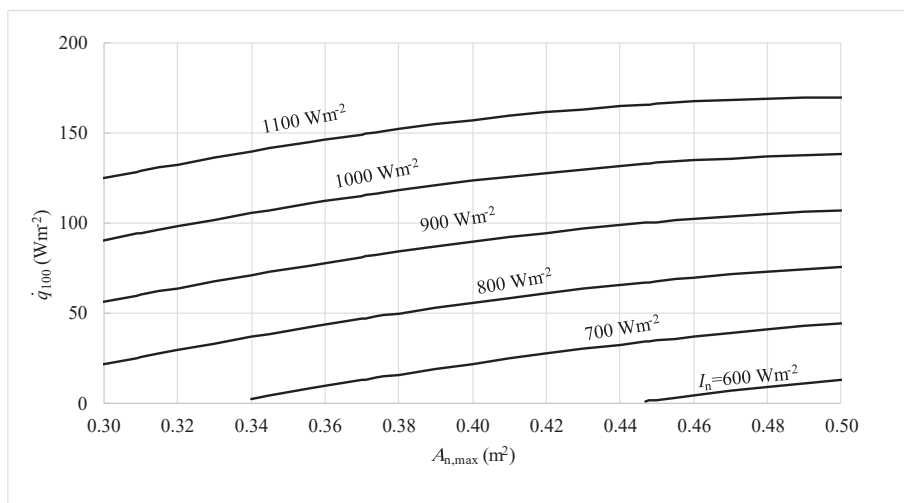


c)

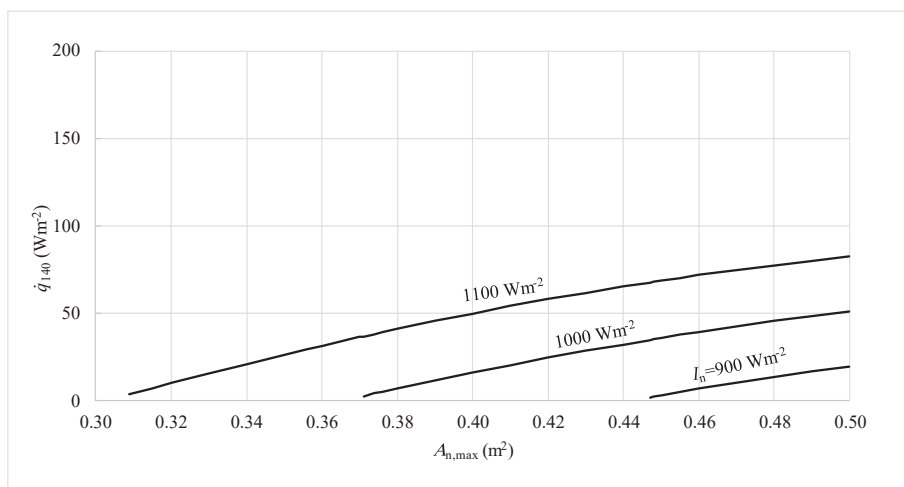
Fig. 12. Influence of cooker aperture area and global solar irradiance on the cooker power: a) \dot{Q}_{65} , b) \dot{Q}_{100} and c) \dot{Q}_{140} .



a)



b)



c)

Fig. 13. Influence of cooker aperture area and global solar irradiance on the specific cooker power: a) \dot{q}_{65} , b) \dot{q}_{100} and c) \dot{q}_{140} .

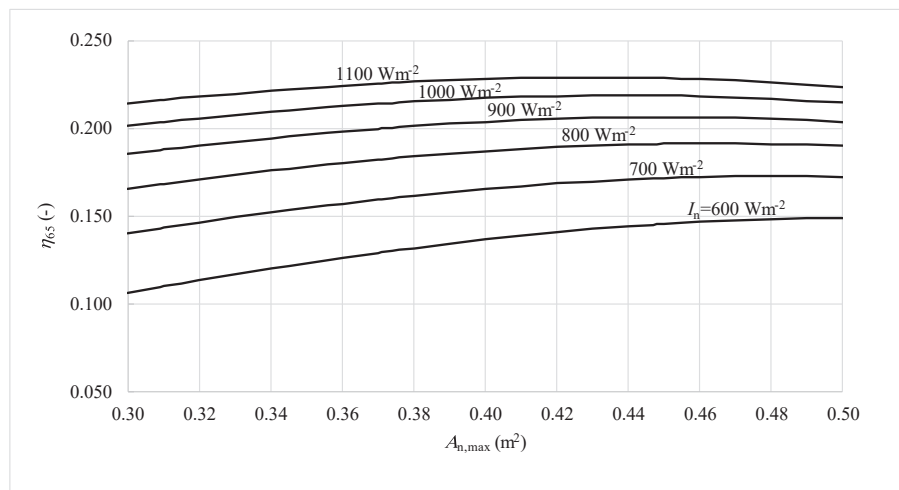


Fig. 14. Influence of cooker aperture area and global solar irradiance on the efficiency η_{65} .

experimental range observed during water heating is too small. Thus, for the funnel cookers tested by Chepkurui and Biira [14], it is impossible to calculate almost of the performance parameters presented in Figs. 10–13.

The new design of solar cooker investigated by Tawfick et al. [4] was tested with and without the bottom cylindrical parabolic reflector also adopting glycerine as load. The mass of glycerine adopted is not directly indicated by the authors [4], but according to the data provided it is estimated to be around 2.14 kg for cooker tested without the bottom reflector. It is higher than the value yet very close to the value adopted in the current study (1.736 kg). According to the plots of Tawfick et al. [4], the time required for glycerine temperature to rise from 50 °C to 95 °C, in the quickest test, is estimated to be 60 min. In the case of the test of current work plotted in Fig. 3, the same time can be estimated to be approximately 36 min and 47 min, respectively, for cookers SC100 and SC70. Tawfick et al. [4] have done some successful tests of real cooking of rice and eggs under real-world conditions. Thus, from the comparison of the results obtained in the present study and the results of Tawfick et al [4], the funnel cooker SC100, with aperture area of 0.5 m², smaller mass of glycerine but with the same load ratio of 3.74 kg m⁻², is faster than the cooker tested by Tawfick et al [4], with aperture area of 0.616 m². The cooker SC100 has been also used, by the author Celestino Rodrigues Ruivo. He has used it regularly for practical family cooking in domestic context, and also in some picnics and some international conferences due to its good portability. It was also designed to fit in a box having the dimensions standardised by the air companies without paying extra luggage costs.

In spite of the load ratio values adopted when testing SC60, SC70, SC80 and SC90 vary from one case to another and are not equal to the value adopted by Tawfick et al. [4], a comparison of COR values is performed. Tawfick et al. [4] reported that the average COR value for the cooker tested without and with the bottom cylindrical parabolic reflector are, respectively, 0.123 and 0.165 m⁻² °C W⁻¹. In the case of current work, the COR ranged from 0.108 to 0.143 m⁻² °C W⁻¹, respectively, for the cookers SC60 and SC100. By using the derived correlation for estimating COR as a function of the aperture area of the funnel cooker, it is estimated that a COR of 0.123 m⁻² °C W⁻¹ would correspond to a funnel cooker with aperture area of 0.39 m². Assuming that the correlation is still valid for aperture area greater than 0.5 m², it is estimated that a COR of 0.165 m⁻² °C W⁻¹ would correspond to a funnel cooker with aperture area of 0.63 m², a value that is close to the area of the cooker tested by Tawfick et al. [4] without the bottom reflector.

It would be also important to extend the presented procedure to

other cookers previously tested with water such as the different configurations of Copenhagen solar cooker [16] and the two configurations of Haines 2 solar cooker [21].

Conclusions

In the current work, funnel solar cookers with five different aperture area configurations ranging from 0.35 to 0.5 m² were tested. The experiments were carried out using the same mass of glycerine as a load in all cases. This implies that each cooker was experimented upon with a different load ratio, a scenario that is not conventional as per the ASAE S580.1 Standard. In each experiment undertaken in the current study, three cookers were tested: a reference cooker having large area and two smaller cookers. Each smaller cooker was tested three times and the reference cooker was tested six times.

The performance curves expressed in terms of efficiency against the specific temperature difference were derived for the five different designs. The optical-thermal ratio of the cooker was determined from the linear derived curve. The reference time of the system associated with each particular tested design was also estimated. The derived correlations of both these parameters were used to estimate the maximum achievable load temperature as well as other performance parameters including the power and the specific power of the cooker as a function of the aperture area, for solar irradiance values from 600 to 1100 W m⁻². Moreover, three selected stages of the heating process, dictated by the load temperature, were selected (65 °C, 100 °C and 140 °C), were considered. Based on the results of the conducted parametric study some findings are summarised:

- It can be affirmed that the pasteurization temperature for the load is achieved even by the design with smallest aperture area, but the boiling point of water at sea level cannot be achieved by the smallest cooker under a low solar irradiance of 600 W m⁻².
- From the plots of the specific power for a temperature difference of 100 °C, it can be estimated that the efficiency of the cooker with an aperture area of 0.5 m² is not far from the value of the cooker with optimum area.
- For a solar irradiance of 1100 W m⁻² and an ambient temperature of 20 °C, the load could theoretically reach a temperature of about 180 °C when the largest cooker configuration is used. Under these almost-perfect conditions, frying will be possible with the largest cooker. Even under a solar irradiance of 800 W m⁻², the largest cooker is expected to achieve boiling temperature of a 1.25 kg of mass of water in a period of 1.6 h when

ambient temperature and initial water temperature are both equal to 20 °C, which is an acceptable indicator for those end-users who can plan their meals timely.

It is important to point out that the calculation methodology adopted in the procedure of deriving the linear performance and evaluating the different parameters was simply and clearly formulated. The mentioned deviations from the recommendations of the ASAE S580.1 Standard protocol should be taken into careful consideration when revising the Standard.

CRedit authorship contribution statement

Celestino Rodrigues Ruivo: Supervision, Conceptualization, Methodology, Formal analysis, Writing – original draft, Writing – review & editing. **Xabier Apaolaza-Pagoaga:** Investigation, Data curation, Visualization, Writing – review & editing. **Antonio Carrillo-Andrés:** Writing – review & editing. **Gianluca Coccia:** Investigation, Writing – review & editing.

Declaration of Competing Interest

The authors declare that they have no known competing financial interests or personal relationships that could have appeared to influence the work reported in this paper.

Data availability

Data will be made available on request.

Appendix A. Data of all tests conducted in the present study

Tables A1 and A2 list the data associated with the experiments conducted during six days to investigate the influence of the effective aperture area on the performance of the funnel solar cooker. The listed time values correspond to solar time. All experiments were conducted using 1.736 kg of glycerine.

Table A1

Data of testing funnel solar cookers SC70, SC90 and SC100 for the set of experiments SetA.

Expt. no.	SetA		
	E141A	E142A	E143A
Day	29 Jun 2021	02 Jul 2021	06 Jul 2021
Start time	10:29	09:38	09:38
End time	14:09	14:38	14:38
Sun elevation angle (°)			
Average value	72	69	69
Minimum value	59	54	54
Maximum value	77	76	76
Solar irradiance I_n (W m ⁻²)			
Average value	1000	990	966
Standard deviation value	9	17	17
Minimum value	975	956	918
Maximum value	1013	1013	995
Ambient temperature (°C)			
Average value	32	29	38
Standard deviation value	0.8	1.1	2.2
Minimum value	28.9	26.6	33.5
Maximum value	33.3	31.1	41.2
Air velocity (m s ⁻¹)			
Average value	0.5	1.0	0.5
Standard deviation value	0.35	0.66	0.36
Minimum value	0	0	0
Maximum value	1.52	2.52	1.51

Table A2

Data of testing funnel solar cookers SC60, SC80 and SC100 for the set of experiments SetB.

Expt. no.	SetB		
	E144A	E145A	E146A
Day	08 Jul 2021	12 Jul 2021	13 Jul 2021
Start time	09:47	10:57	09:37
End time	13:37	15:37	14:37
Sun elevation angle (°)			
Average value	71	68	68
Minimum value	58	41	53
Maximum value	76	75	75
Solar irradiance I_n (W m ⁻²)			
Average value	958	940	966
Standard deviation value	72	11	14
Minimum value	546	861	904
Maximum value	1007	960	1001
Ambient temperature (°C)			
Average value	29	41	31
Standard deviation value	0.9	0.9	0.8
Minimum value	27.1	38.5	28.8
Maximum value	31.2	42.7	33.3
Air velocity (m s ⁻¹)			
Average value	1.0	0.5	0.5
Standard deviation value	0.55	0.40	0.58
Minimum value	0	0	0
Maximum value	3.02	2.01	3.02

References

- [1] Sagade AA, Samdarshi SK, Panja PS. Enabling rating of intermediate temperature solar cookers using different working fluids as test loads and its validation through a design change. *Sol Energy* 2018;171:354–65. <https://doi.org/10.1016/j.solener.2018.06.088>.
- [2] Sagade AA, Apaolaza-Pagoaga X, Rodrigues Ruivo C, Carrillo-Andrés A. Concentrating solar cookers in urban areas: Establishing usefulness through realistic intermediate temperature rating and grading. *Sol Energy* 2022;241:157–66. <https://doi.org/10.1016/j.solener.2022.06.007>.
- [3] Khallaf AM, Tawfik MA, El-Sebaai AA, Sagade AA. Mathematical modeling and experimental validation of the thermal performance of a novel design solar cooker. *Sol Energy* 2022;207:40–50. <https://doi.org/10.1016/j.solener.2020.06.069>.
- [4] Tawfik MA, Sagade AA, Palma-Behnke R, Abd Allah WE, Hanan ME. Solar cooker with tracking-type bottom reflector: An experimental thermal performance evaluation of a new design. *Sol Energy* 2021;220:295–315. <https://doi.org/10.1016/j.solener.2021.03.063>.
- [5] Solar panel cooker designs, SCI Solar cookers international https://solarcooking.fandom.com/wiki/Category:Solar_panel_cooker_designs (Accessed 3 May 2022).
- [6] HotPot user's guide, Solar Household Energy. <https://www.she-inc.org/wp-content/uploads/2014/02/userguide.pdf> (Accessed 3 May 2022).
- [7] Ruivo C, Carrillo-Andrés A, Apaolaza-Pagoaga X. Experimental determination of the standardised power of a solar funnel cooker for low sun elevations. *Renew Energy* 2021;170:364–74. <https://doi.org/10.1016/j.renene.2021.01.146>.
- [8] Apaolaza-Pagoaga X, Carrillo-Andrés A, Ruivo C. New approach for analysing the effect of minor and major solar cooker design changes: influence of height trivet on the power of a funnel cooker. *Renew Energy* 2021;179:2071–85. <https://doi.org/10.1016/j.renene.2021.08.025>.
- [9] Apaolaza-Pagoaga X, Sagade AA, Rodrigues Ruivo C, Carrillo-Andrés A. Performance of solar funnel cookers using intermediate temperature test load under low sun elevation. *Sol Energy* 2021;225:978–1000. <https://doi.org/10.1016/j.solener.2021.08.006>.
- [10] Carrillo-Andrés A, Apaolaza-Pagoaga X, Rodrigues Ruivo C, Rodríguez-García E, Fernández-Hernández F. Optical characterization of a funnel solar cooker with azimuthal sun tracking through ray-tracing simulation. *Sol Energy* 2022;233:84–95. <https://doi.org/10.1016/j.solener.2021.12.027>.
- [11] ASAE S580.1 NOV2013, Testing and reporting solar cooker performance, American Society of Agricultural Engineers, Michigan, USA, 2013.
- [12] Test Results, Solar Cookers International. <https://www.solarcookers.org/work/research/results> (Accessed 3 May 2022).
- [13] Ebersviller SM, Jetter JJ. Evaluation of performance of household solar cookers. *Sol Energy* 2020;208:166–72. <https://doi.org/10.1016/j.solener.2020.07.056>.
- [14] Chepkurui J, Biira S. Thermal performance evaluation of the funnel solar cooker of different funnel lengths implemented in Nagongera, Uganda. *Tanzan J Sci* 2020;46:53–60.
- [15] Regattieri A, Piana F, Bortolini M, Gamberi M, Ferrari E. Innovative portable solar cooker using the packaging waste of humanitarian supplies. *Renew Sustain Energy Rev* 2016;57:319–26. <https://doi.org/10.1016/j.rser.2015.12.199>.
- [16] Apaolaza-Pagoaga X, Carrillo-Andrés A, Ruivo CR. Experimental thermal performance evaluation of different configurations of Copenhagen solar cooker. *Renew Energy* 2022;184:604–18. <https://doi.org/10.1016/j.renene.2021.11.105>.

- [17] J.A. Duffie, W.A. Beckman, *Solar Engineering of Thermal Processes*, fourth ed., Wiley, 2013.
- [18] Ruivo C, Apaolaza-Pagoaga X, Di Nicola G, Carrillo-Andrés A. On the use of experimental measured data to derive the linear regression usually adopted for determining the performance parameters of a solar cooker. *Renew Energy* 2022; 181:105–15. <https://doi.org/10.1016/j.renene.2021.09.047>.
- [19] Ruivo C, Apaolaza-Pagoaga X, Coccia G, Carrillo-Andrés A. Proposal of a non-linear curve for reporting the performance of solar cookers. *Renew Energy* 2022;191: 110–21. <https://doi.org/10.1016/j.renene.2022.04.026>.
- [20] Coccia G, Di Nicola G, Pierantozzi M, Tomassetti S, Aquilanti A. Design, manufacturing, and test of a high concentration ratio solar box cooker with multiple reflectors. *Sol Energy* 2017;155:781–92. <https://doi.org/10.1016/j.solener.2017.07.020>.
- [21] Apaolaza-Pagoaga X, Carrillo-Andrés A, Ruivo CR. Experimental characterization of the thermal performance of the Haines 2 solar cooker. *Energy* 2022;257:124730. <https://doi.org/10.1016/j.energy.2022.124730>.